CrossMark
click for updates

Enoyl-Acyl Carrier Protein Reductase I (FabI) Is Essential for the Intracellular Growth of *Listeria monocytogenes*

Jiangwei Yao, Megan E. Ericson, Matthew W. Frank, Charles O. Rock

Department of Infectious Diseases, St. Jude Children's Research Hospital, Memphis, Tennessee, USA

Enoyl-acyl carrier protein reductase catalyzes the last step in each elongation cycle of type II bacterial fatty acid synthesis and is a key regulatory protein in bacterial fatty acid synthesis. Genes of the facultative intracellular pathogen *Listeria monocytogenes* encode two functional enoyl-acyl carrier protein isoforms based on their ability to complement the temperature-sensitive growth phenotype of *Escherichia coli* strain JP1111 [*fabI*(Ts)]. The FabI isoform was inactivated by the FabI selective inhibitor AFN-1252, but the FabK isoform was not affected by the drug, as expected. Inhibition of FabI by AFN-1252 decreased endogenous fatty acid synthesis by 80% and lowered the growth rate of *L. monocytogenes* in laboratory medium. Robust exogenous fatty acid incorporation was not detected in *L. monocytogenes* unless the pathway was partially inactivated by AFN-1252 treatment. However, supplementation with exogenous fatty acids did not restore normal growth in the presence of AFN-1252. FabI inactivation prevented the intracellular growth of *L. monocytogenes*, showing that neither FabK nor the incorporation of host cellular fatty acids was sufficient to support the intracellular growth of *L. monocytogenes*. Our results show that FabI is the primary enoyl-acyl carrier protein reductase of type II bacterial fatty acid synthesis and is essential for the intracellular growth of *L. monocytogenes*.

*L*isteria monocytogenes is a facultative intracellular Gram-positive bacterium that is the primary cause of the disease listeriosis (1). The environmentally hardy and ubiquitous *L. monocytogenes* is ingested through contaminated food products and can cause noninvasive diseases, such as gastroenteritis, or invade through the intestinal epithelium to cause central nervous system infections or bacteremia. *L. monocytogenes* poses a major medical threat for pregnant women and immunocompromised patients. Yearly outbreaks of *L. monocytogenes* in a variety of food products from fruits to ice cream underscore the need to understand the requirements for *L. monocytogenes* infection and discover new methods to inhibit the growth of *L. monocytogenes*.

The phospholipids of *L. monocytogenes* are composed of branched-chain fatty acids synthesized by the *L. monocytogenes* type II fatty acid synthesis system. Decreasing the synthesis of branched-chain fatty acids by the genetic deletion of the branched-chain α-keto acid dehydrogenase compromises the environmental survival and intracellular pathogenesis of *L. monocytogenes* (2–6). The pathways for fatty acid synthesis, phospholipid synthesis, and exogenous fatty acid incorporation of *L. monocytogenes* are predicted to be the same as those for the phylogenetically related and well-characterized *Staphylococcus aureus* system (Fig. 1). Fatty acids are synthesized using a prototypical type II bacterial fatty acid synthesis, with 2-methylbutyryl-coenzyme A (CoA) as the primer, to make branch-chain fatty acids (3, 5, 7–9). An acyl-acyl carrier protein (ACP) of the appropriate length is used as the acyl donor by the PlsX/Y/C system to make phosphatidic acid from glycerol-3-phosphate (10, 11). Exogenous fatty acids are incorporated via the fatty acid kinase system (12–14). An unusual feature of *L. monocytogenes* fatty acid synthesis is the presence of four genes that may encode enoyl-acyl carrier protein reductases, including a FabI, a FabL, and two FabK isoforms, rather than the single FabI found in *S. aureus* and a variety of other bacterial pathogens. The FabL isoform was discovered in the phylogenetically related *Bacillus*, which also has a FabI (15). Both proteins function in fatty acid synthesis in *Bacillus*. The FabK isoform is a flavoprotein unrelated

to FabI that was originally discovered in *Streptococcus pneumoniae* (16). The *Enterococcus faecalis* genome encodes both FabI and FabK, but FabI is responsible for the bulk of fatty acid synthesis while FabK plays a minor role in supporting fatty acid synthesis (17).

The goal of this study was to identify which of the putative *L. monocytogenes* reductase genes code for functional enoyl-acyl carrier protein reductases, assess their contribution to supporting type II bacterial fatty acid synthesis, and determine their role in planktonic and intracellular growth. Complete inhibition of FabI using the FabI selective inhibitor AFN-1252 reduced the fatty acid synthesis of *L. monocytogenes* strain 10403S by 80% and reduced the growth rate of *L. monocytogenes* in laboratory medium. In contrast, FabI inactivation through AFN-1252 stopped the intracellular growth of *L. monocytogenes*. These results establish that FabI is the major enoyl acyl carrier protein reductase of type II fatty acid synthesis and that FabI-dependent type II fatty acid synthesis is essential for the intracellular growth of *L. monocytogenes* and validates FabI as an effective drug target against intracellular *L. monocytogenes*.

MATERIALS AND METHODS

Materials. Chemicals were from Fisher Scientific or Sigma-Aldrich. Bacterial medium supplies were from BD Medical Technology, while human cell culture supplies were from Life Technologies. Radioactive chemicals
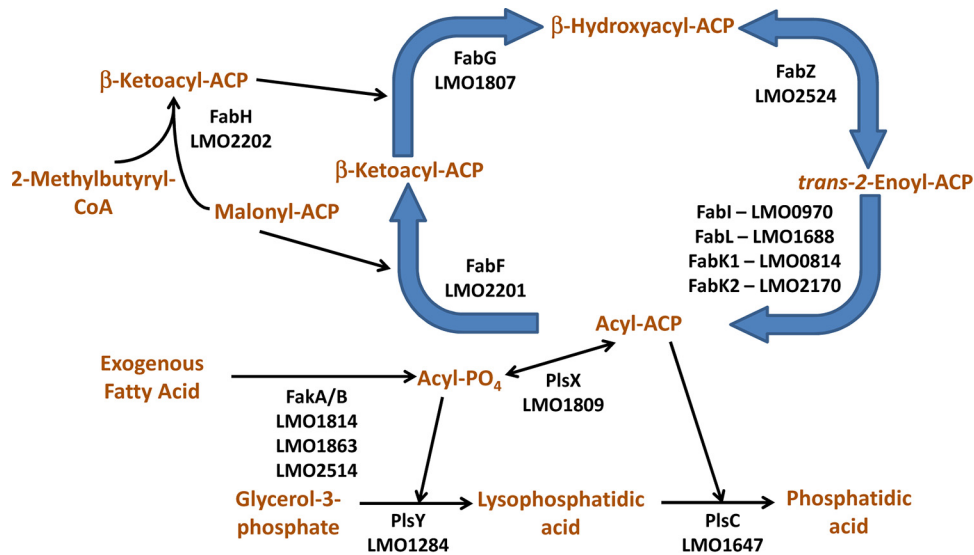
FIG 1 Fatty acid synthesis, phospholipid synthesis, and exogenous fatty acid incorporation system of *L. monocytogenes*. The locus tags for the genes in *L. monocytogenes* strain EGD-e are annotated below the enzyme symbols. The *L. monocytogenes* genome encodes the same basic type II bacterial fatty acid synthesis, acyltransferase, and exogenous fatty acid incorporation system as the characterized *S. aureus* system. The unique aspect of *L. monocytogenes* is that the *L. monocytogenes* genome has four putative enoyl-acyl carrier protein reductase genes of three different isoforms. The gene LMO0970 is predicted to encode the FabI isoform (53% identity; E value of $1e^{-89}$ versus FabI from *S. aureus*). The gene LMO1688 is predicted to encode the FabL isoform (69% identity; E value of $1e^{-120}$ versus FabL from *B. subtilis*). The gene LMO0814 is predicted to encode the FabK isoform (50% identity; E value of $1e^{-100}$ versus FabK from *S. pneumoniae*). The gene LMO2170 is also predicted to encode the FabK isoform (51% identity; E value of $7e^{-99}$ versus FabK from *S. pneumoniae*).

were from American Radiolabeled Chemicals, and [7,7,8,8-D4]palmitic acid (D4-16:0) was from Cambridge Isotope Laboratories.

Bacterial growth. *L. monocytogenes* strain 10403S was grown in brain heart infusion medium for routine growth and maintenance. *L. monocytogenes* was grown in tryptic soy broth for growth inhibition, pathway labeling, and exogenous fatty acid supplementation experiments because tryptic soy broth lacked the exogenous fatty acids in brain heart infusion medium. *L. monocytogenes* was grown at 37°C with shaking at 200 rpm unless otherwise indicated.

Molecular biology. The predicted *L. monocytogenes* FabI (*Lm*FabI; LMO0970), *Lm*FabL (LMO1688), *Lm*FabK1 (LMO0814), and *Lm*FabK2 (LMO2170) proteins were optimized for expression in *Escherichia coli* through GeneArt gene synthesis technology (Life Technologies). An NdeI restriction site was engineered at the 5′ end of the gene with the start codon in the NdeI restriction site, while a stop codon and an EcoRI restriction site were engineered at the 3′ end of the gene. The genes were cloned into the plasmid pPJ131. The pPJ131 plasmid is a pBluescript plasmid (Stratagene) containing the multiple-cloning site from pPET28a for protein expression in *E. coli* (18, 19). The resulting expressed protein has an N-terminal histidine tag from the pET28a multiple-cloning site. The polyhistidine tag allows for the detection and purification of the expressed protein. Although tags sometimes affect protein function, there are no examples of histidine tags interfering with FabI or FabK activity. The protein encoded by the plasmid is constitutively expressed because the pPJ131 plasmid is a high-copy-number plasmid, and the endogenous *lacI* is titrated by copy number.

Complementation. The expression constructs containing the four putative *L. monocytogenes* enoyl-acyl carrier protein reductases (LMO0814, LMO0970, LMO1688, and LMO2170) were transformed into the *fabI* temperature-sensitive *E. coli* strain JP1111 [*fabI*(Ts)] to determine complementation. The pPJ131 parent plasmid was used as a negative complementation control, and the pPJ131 plasmid expressing FabI from *S. aureus* was used as the positive control (20). Strain JP1111 is able to grow at 30°C but was nonviable at 42°C without FabI complementation.

Western blotting. JP1111 cells harboring plasmids containing LMO0814, LMO0970, LMO1688, and LMO2170 were grown at 30°C in

lysogeny broth to an A_{600} of 1. The cells were washed twice with phosphate-buffered saline and harvested via centrifugation. The cells were resuspended in B-PER bacterial protein extraction reagent (1 ml per 25-ml culture; Thermo Scientific) and shaken for 30 min to lyse the cells. The resulting mixture was centrifuged at 20,000 × *g* to separate the supernatant from the cellular debris. Equal volumes of the supernatant from each expression strain were electrophoresed on a NuPAGE Novex 10% Bis-Tris protein gel (Life Technologies), and protein expression was visualized via Western blot analysis using a primary rabbit polyclonal IgG His-probe antibody (Santa Cruz Biotechnology) (21) and a secondary goat alkaline phosphatase-linked anti-rabbit IgG antibody (Sigma-Aldrich) (20). The blot was visualized using ECF substrate (GE Healthcare) on a Typhoon FLA 9500 imager in the fluorescence detection mode.

Susceptibility of *L. monocytogenes* enoyl-acyl carrier protein reductase to AFN-1252. The *L. monocytogenes* enoyl-acyl carrier protein reductase genes that complemented the growth of JP1111 were transformed into *E. coli* strain ANS1 (Δ*tolC*), an efflux pump-deficient *E. coli* strain with increased susceptibility to AFN-1252 (20). The AFN-1252 MIC against ANS1 expressing the parent pPJ131 plasmid, the pPJ131 plasmid expressing the *S. aureus fabI* gene, and the pPJ131 plasmid expressing the functional *L. monocytogenes* enoyl-acyl carrier protein reductase genes was determined to evaluate the susceptibility of the *L. monocytogenes* enoyl-acyl carrier protein reductases to AFN-1252.

Growth experiments. *L. monocytogenes* was cultured overnight in tryptic soy broth medium. The overnight culture was back diluted to an A_{600} of 0.02 in tryptic soy broth medium, and the A_{600} was monitored over 5 h for AFN-1252 in growth rate experiments. The overnight culture was back diluted to an A_{600} of 0.02 in tryptic soy broth medium with 0.1% Brij-58 in fatty acid growth complementation experiments. Fatty acids are known to have inhibitory effects on the growth of *L. monocytogenes* (22), but delivering fatty acids in the detergent Brij-58 (0.1%) overcomes the inhibitory effects (23, 24). The culture was grown until an A_{600} of ≈0.05 and split into six 14-ml aliquots: dimethyl sulfoxide (DMSO) only added, DMSO with 100 μM D4-16:0 and 100 μM 18:1, DMSO with 100 μM anteiso-15:0 and 100 μM anteiso-17:0, 50 μM AFN-1252, 50 μM AFN-1252 with 100 μM D4-16:0 and 100 μM 18:1, and 50 μM AFN-1252 with 100 μM anteiso-15:0 and 100 μM anteiso-17:0. Growth was monitored

over 5 h or until the A_{600} becomes greater than 1.5. After 5 h or an A_{600} of >1.5 was reached, 2.5 ml of the culture was harvested, washed with phosphate-buffered saline, extracted for lipids via the Bligh and Dyer method (25), and analyzed via molecular species analysis to determine the phospholipid species (24, 26). Growth curves and molecular species analysis experiments were conducted on two independent biological replicates, and representative curves and spectra are shown in the figures.

Acetate labeling experiments. *L. monocytogenes* was cultured overnight in tryptic soy broth medium. The overnight culture was back diluted to an A_{600} of 0.1 in tryptic soy broth medium and grown to an A_{600} of 0.4. The culture was split into 5-ml aliquots, and the aliquots were incubated with a final concentration of 0, 0.04, 0.15, 0.6, 2.5, 10, and 50 μM AFN-1252 for 15 min. [^{14}C]acetate (5 μCi) was added to each aliquot and incubated for 45 min. The cells were pelleted via centrifugation and washed twice with phosphate-buffered saline, and the lipids were isolated (25). The amount of [^{14}C]acetate incorporated into the phospholipids was measured via liquid scintillation counting (Tri-Carb 2910 TR; PerkinElmer Life Sciences). Data were plotted as the fraction of incorporation compared to that of the untreated cells and fitted via a 50% inhibitory concentration (IC_{50}) equation with partial inhibition in GraphPad Prism 5.

Pathway labeling experiments. *L. monocytogenes* was cultured overnight in tryptic soy broth medium. The overnight culture was back diluted to an A_{600} of 0.1 in tryptic soy broth medium and grown to an A_{600} of 0.4. The culture was split into 10-ml aliquots, and the aliquots were incubated with a final concentration of 0.5% DMSO or 50 μM AFN-1252 for 15 min. The aliquots then were labeled for 45 min with 10 μCi of an ^{3}H-labeled L-amino acid mixture, [^{3}H]thymidine, or [^{3}H]uracil to measure protein, DNA, and RNA synthesis, respectively. The cells were harvested via filtration and washed with 3 ml of phosphate-buffered saline 3 times. The filters were incubated with the liquid scintillation solution for 2 h, and the radioactive incorporation into the cells was measured via liquid scintillation counting of the filter. Data are plotted as fractional incorporation relative to the untreated cells normalized to the final A_{600} of the cultures. Plotted data were derived from two biological replicates. The statistical significance of whether each pathway was inhibited by AFN-1252 was determined using Student's *t* test.

Intracellular infection. *L. monocytogenes* strain 10403S was used to infected HeLa cells as previously described (27). Briefly, *L. monocytogenes* was grown overnight in brain heart infusion medium at 37°C with shaking at 200 rpm. The culture was back diluted to an A_{600} of 0.25 in brain heart infusion medium and grown for 1 h. *L. monocytogenes* was washed with phosphate-buffered saline and resuspended in DMEM (Dulbecco's modified Eagle medium with 10% fetal bovine serum) at the appropriate concentration such that 2 ml of medium per well gave the desired multiplicity of infection (MOI). HeLa cell monolayers grown to 80% confluence in 6-well plates (ca. 1×10^6 HeLa cells per well) were washed twice with Hanks' balanced salt solution (HBSS). *L. monocytogenes* resuspended in DMEM was added to the HeLa cells. The plates were centrifuged at 900 × *g* for 15 min at room temperature and then incubated for 105 min at 37°C in 5% CO_2. Cells next were washed 2 times with HBSS and incubated in 2 ml of DMEM and 40 μg/liter gentamicin for 60 min. The cells were washed 2 more times with HBSS and incubated in DMEM and 40 μg/liter gentamicin (and DMSO or AFN-1252 where appropriate) at 37°C in 5% CO_2 until ready for use. For microscopy experiments, glass coverslips were placed at the bottom of the well, and the HeLa cells were seeded onto the coverslips. All other infection and growth procedures remained the same. Growth curve and mass spectrometry experiments were conducted at an MOI of 1, while microscopy experiments were conducted at an MOI of 15.

The number of *L. monocytogenes* organisms per well was determined by lysing the HeLa cells and observing the number of CFU of *L. monocytogenes*. Briefly, the infected HeLa cells were washed with HBSS twice and resuspended in HBSS. The cells were resuspended via cell scraping, collected into microcentrifuge tubes, and resuspended in 0.1% Triton X-100

on ice. The solution was alternately vortexed thoroughly and incubated on ice for 20 min to lyse the HeLa cells to free the intracellular *L. monocytogenes*. The solution was serially diluted in brain heart infusion medium and plated on brain heart infusion medium agar plates to determine the CFU per well. For intracellular growth curve experiments, the infected HeLa cells were lysed immediately after infection (0 h), 3.5 h after infection, 20 h after infection, and 44 h after infection. The cells were collected via scraping and then washed twice with phosphate-buffered saline before lipid extraction and analysis for mass spectrometry experiments.

Molecular species analysis. Phospholipid molecular species fingerprints were determined using direct infusion electrospray ionization-mass spectrometry technology. Mass spectrometry analysis was performed using a QTrap 4500 (Sciex, Framingham, MA) equipped with a Turbo V ion source. Lipid extracts were resuspended in 50:50 (vol/vol) chloroform-methanol plus 1% formic acid. The instrument was operated in the negative ion mode for phosphatidylglycerol (PG), phosphatidylinositol (PI), and fatty acid scan analysis. The ion source parameters were the following: ion spray voltage, −4,500 V; curtain gas, 15 lb/in^2; temperature, 270°C; collision gas, medium; ion source gas 1, 15 lb/in^2; and ion source gas 2, 25 lb/in^2. Parameters for PG analysis were the following: scan range, 600 to 900 m/z; declustering potential, −30 V; collision energy, −45 V; peak width, Q1 and Q3 0.7 FWHM (full width at half maximum). For PI and 15:0 fatty acid analysis, lipid classes were separated using a Discovery DSC-NH2 solid-phase extraction column (Supelco, Bellefonte, PA). In brief, the column was conditioned with 8 ml of hexane and lipid extract was added. Nonpolar lipids were eluted with 6 ml of 2:1 (vol/vol) chloroform-isopropyl alcohol, fatty acids were eluted with 6 ml of ether plus 2% acetic acid, phosphatidylcholine and phosphatidylethanolamine were eluted with 6 ml of methanol, and phosphatidylglycerol and phosphatidylinositol were eluted with 6 ml of chloroform–methanol–0.8 M sodium acetate (60:30:4.5, vol/vol/vol). PI and 15:0 fatty acid parameters were the following: precursor ion, 241 m/z; scan range, 600 to 1,000 m/z; declustering potential, −35 V; collision energy, −40 V; peak width, Q1 and Q30.7 FWHM.

Microscopy. The DMSO- or AFN-1252-treated infected HeLa cells were visualized via immunofluorescence microscopy. Glass coverslips in the 6-well plates were washed twice with phosphate-buffered saline and then fixed with 4% formaldehyde and 2% goat serum in phosphate-buffered saline. Hydration chambers were constructed from 150-mm petri dishes. Coverslips were washed with phosphate-buffered saline five times and placed in hydration chambers. Cells were permeabilized with 300 μl of 0.1% NP-40, 2% goat serum in phosphate-buffered saline for 10 min at room temperature and washed with phosphate-buffered saline five times. The samples were then blocked with 10% goat serum in phosphate-buffered saline for 30 min at room temperature. The blocking solution was aspirated and the samples were incubated with the primary rabbit anti-*Listeria* antibody (1:1,000 dilution of stock AB35132 from AbCam [28, 29]) in 2% goat serum, 0.1% NP-40, and phosphate-buffered saline for 1 h at room temperature. The sample was washed 5 times with phosphate-buffered saline and then incubated with anti-rabbit antibody conjugated to Alexa Fluor-488 (1:1,000 dilution of stock from Thermo Fisher) in 2% goat serum, 0.1% NP-40, and phosphate-buffered saline for 1 h at room temperature in the dark. In experiments with 4′,6-diamidino-2-phenylindole (DAPI), 1 μg/ml of dye was added with secondary antibody. Samples were washed five times with phosphate-buffered saline. In experiments with Alexa Fluor 594-conjugated phalloidin (Thermo Fisher), 200 μl of 100 nM phalloidin was added and incubated in the dark at room temperature for 15 min, and then samples were washed five times with phosphate-buffered saline. Samples were mounted in FluorSave (Calbiochem), dried overnight, and sealed with nail polish. High-resolution images looking at the intracellular shape of the bacteria were taken using a Zeiss LSM 780 microscope and Zeiss Zen software. Other images were taken using an Olympus BX41 using SPOT imaging software. The number of *Listeria monocytogenes* cells per HeLa nuclei from 3 representative fields containing at least 100 HeLa nuclei was determined for AFN-1252- and

DMSO-treated *Listeria monocytogenes*-infected HeLa cells. The statistical significance between the two treatment groups was determined using Student's *t* test.

RESULTS

The genome of *L. monocytogenes* encodes two enoyl-acyl carrier protein reductase isoforms. Enoyl-acyl carrier protein reductase catalyzes the reduction of *trans*-2-enoyl-ACP to acyl-ACP using the reducing potential of NAD(P)H in the last, rate-determining reaction of the elongation cycle (30, 31). Several isoforms of enoyl-acyl carrier protein reductase are known in bacteria. FabI is the first discovered isoform and is a member of the short-chain dehydrogenase/reductase protein family (32). The FabL isoform also belongs to the short-chain dehydrogenase/reductase protein family but is structurally divergent from FabI (15). FabL was discovered in *Bacillus*, which also expresses FabI. The FabK isoform is a flavoprotein unrelated to FabI and FabL. It was originally discovered in *S. pneumoniae* (16) and is found predominantly in other Gram-positive bacteria. The FabV isoform is found only in select Gram-negative bacteria (33, 34).

FabI from *S. aureus*, FabL from *Bacillus subtilis*, FabK from *S. pneumoniae*, and FabV from *Vibrio cholerae* were used to search the *L. monocytogenes* genome for related proteins. The *L. monocytogenes* genome encoded four enoyl-acyl carrier protein reductase gene homologues (Fig. 1 and NCBI Microbial Genome Resources). The LMO0970 gene encodes a putative FabI, the LMO1688 gene encodes a putative FabL, and the LMO0814 and LMO2170 genes encode putative FabKs. None of these genes are neighbored by another fatty acid metabolism gene. These bioinformatics predictions were validated experimentally because *S. aureus* and *Bacillus subtilis* encode FabK homologues that do not possess enoyl-acyl carrier protein reductase function (16). Whether these genes can function as enoyl-acyl carrier protein reductases was tested by assessing if the expression of these genes, using a constitutive promoter on a multicopy plasmid, complemented the growth of the temperature-sensitive *E. coli* strain JP1111 [*fabI*(Ts)] (35). *Lm*FabI (LMO0970) and *Lm*FabK1 (LMO0814) complemented the growth of JP1111 at the nonpermissive temperature, while *Lm*FabL (LMO1688) weakly complemented growth at the nonpermissive temperature (Fig. 2A and B). *Lm*FabK2 (LMO2170) expression did not restore the growth of the temperature-sensitive strain. The expression of the four predicted *L. monocytogenes* enoyl-acyl carrier protein reductases in the JP1111 cells was verified to ensure that the inability to complement was due to the lack of enoyl-acyl carrier protein reductase activity rather than lack of protein expression. All four proteins were expressed in JP1111 cells (Fig. 2C), showing that that *Lm*FabI and *Lm*FabK1 were the two most active enoyl-acyl carrier protein reductases encoded by *L. monocytogenes* genes.

Validation of AFN-1252. AFN-1252 is a potent and selective inhibitor of FabI that has no known off-target effects (20, 24, 36, 37). AFN-1252 inhibits the growth of bacteria with a single essential FabI, including intracellular pathogens (18, 20, 24, 38), but is ineffective against bacterial genes encoding the other enoyl-acyl carrier protein reductase isoforms (39). These data, coupled with the observation that *S. aureus accD* mutants are refractory to AFN-1252 (14), show there is little or no off-target toxicity of this drug. Therefore, AFN-1252 was used as a tool to determine the contribution of *Lm*FabI versus *Lm*FabK1 to fatty acid synthesis and growth of *L. monocytogenes*. AFN-1252 was tested against *E. coli*
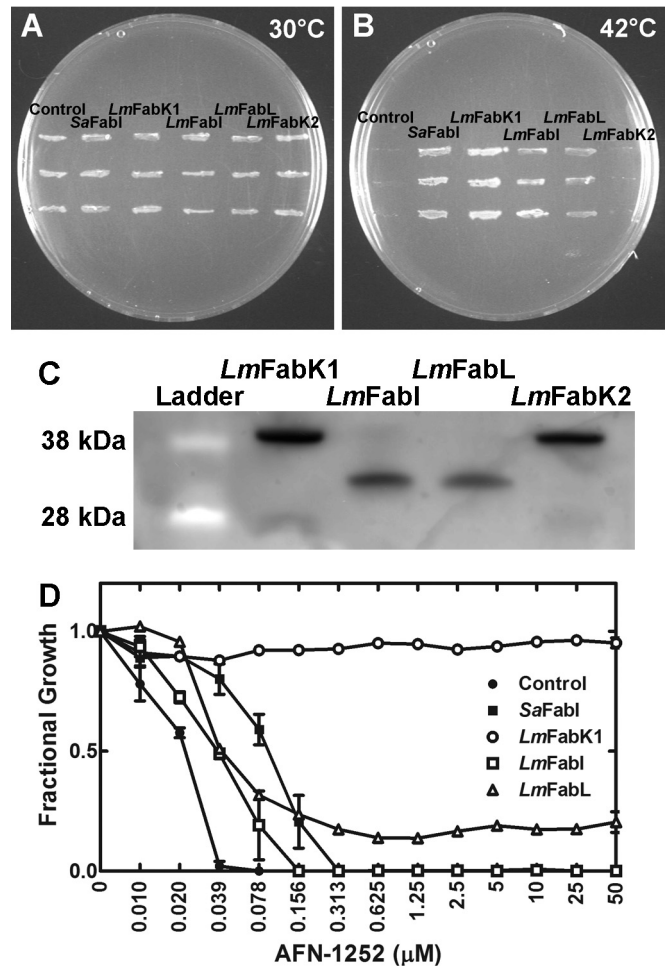
FIG 2 *L. monocytogenes* encodes two functional enoyl-acyl carrier protein reductase isoforms. (A) Growth of the temperature-sensitive *E. coli* strain JP1111 [*fabI*(Ts)] transformed with the empty plasmid (Control) or plasmids expressing either *S. aureus* FabI (*Sa*FabI), predicted *L. monocytogenes* FabK1 (*Lm*FabK1; LMO0814), predicted *L. monocytogenes* FabI (*Lm*FabI; LMO0970), predicted *L. monocytogenes* FabL (*Lm*FabL; LMO1688), or predicted *L. monocytogenes* FabK2 (*Lm*FabK2; LMO2170) under the permissive growth condition (30°C). (B) Growth of the same strains at the nonpermissive temperature (42°C). (C) The expression of the predicted *L. monocytogenes* enoyl-acyl carrier protein reductases in JP1111 was verified via Western blot analysis. JP1111 cells expressing the enoyl-acyl carrier protein reductases were grown at 30°C to an A_{600} of 1. The cells were lysed, and the supernatant was separated from the cell debris. Western blot analysis against the supernatant fraction using an antihistidine tag was performed to ensure that the predicted enoyl-acyl carrier protein reductase was expressed. All four predicted enoyl-acyl carrier protein reductases (*Lm*FabK1, 32.4 kDa; *Lm*FabI, 28.3 kDa; *Lm*FabL, 27.2 kDa; *Lm*FabK2, 32.5 kDa; each with 2.1 kDa added from the N-terminal histidine tag from pPJ131 plasmid) were expressed in JP1111. Data shown as a representative blot are from 2 biological replicates. (D) MIC of AFN-1252 against the *E. coli* strain ANS1 (Δ*tolC*) expressing empty plasmid (control), *S. aureus* FabI (*Sa*FabI), *L. monocytogenes* FabK (*Lm*FabK1; LMO0814), *L. monocytogenes* FabI (*Lm*FabI; LMO0970), and *L. monocytogenes* FabL (*Lm*FabL; LMO1688).

strain ANS1 (Δ*tolC*), expressing *Lm*FabI, *Lm*FabK1, or *Lm*FabL. Strain ANS1, harboring the empty plasmid (control), had an AFN-1252 MIC of 0.039 μM, whereas the MIC in the strain expressing *S. aureus* FabI (*Sa*FabI) increased by 8-fold to 0.313 μM (Fig. 2D). Strain ANS1, expressing *Lm*FabI, had an AFN-1252
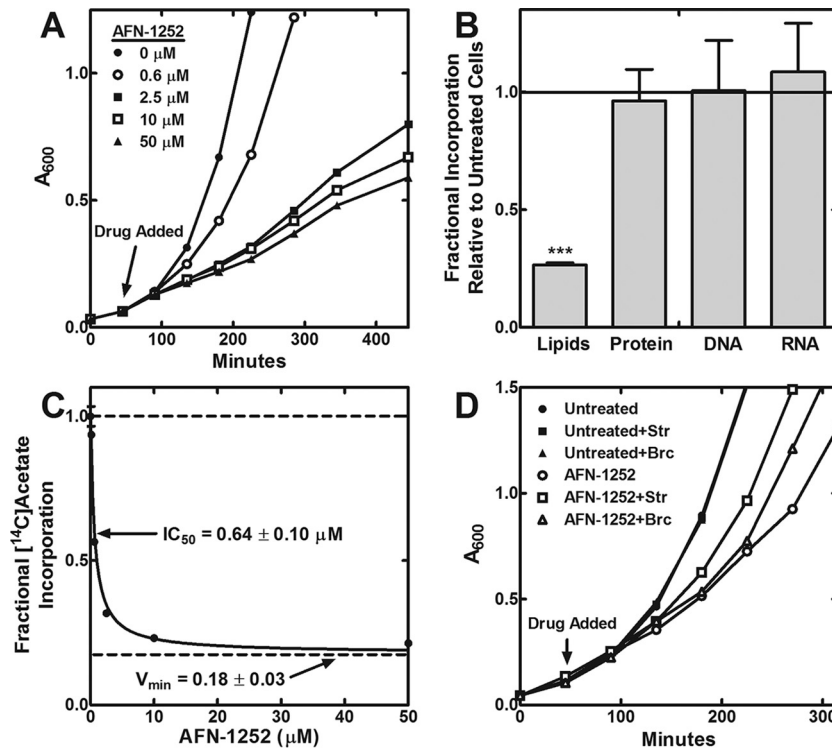
FIG 3 AFN-1252 causes on-target, partial inhibition of phospholipid synthesis of *L. monocytogenes*. (A) The effect of increasing concentrations of AFN-1252 on the growth of *L. monocytogenes* in tryptic soy broth medium. AFN-1252 was added to cells at the time indicated by the arrow. The growth curve shown is representative of duplicate biological replicates. (B) The effect of AFN-1252 on the major biosynthetic pathways was measured by treating growing *L. monocytogenes* cells with 50 μM AFN-1252 and comparing them to untreated cells. Metabolic labeling with [^{14}C]acetate was used for lipid biosynthesis, an ^{3}H-labeled L-amino acid mixture was used to measure protein biosynthesis, [^{3}H]thymidine incorporation measured DNA biosynthesis, and [^{3}H]uracil measured stable RNA biosynthesis, as described in Materials and Methods. Data shown are averages with standard deviations from two biological replicates. Lipid biosynthesis was the only pathway inhibited by AFN-1252. Significance was determined using Student's *t* test. ***, $P < 0.001$. (C) AFN-1252 inhibition of [^{14}C]acetate incorporation into the phospholipids of *L. monocytogenes* in tryptic soy broth medium. The fractional [^{14}C]acetate incorporation was compared to that of the no-inhibitor control. Data shown are averages with standard deviations from two biological replicates. The data were fit to an IC$_{50}$ equation with partial inhibition. The IC$_{50}$ is the concentration of AFN-1252 needed to inhibit 50% of the sensitive fatty acid synthesis activity. V$_{min}$ is the fraction of residual fatty acid synthesis activity that could not be inhibited by AFN-1252. (D) The effect of branched-chain fatty acid (Brc; 100 μM anteiso-15:0 and 100 μM anteiso-17:0) and straight-chain fatty acid (Str; 100 μM D4-16:0 and 100 μM 18:1) supplementation on AFN-1252 inhibition of *L. monocytogenes* growth in tryptic soy broth medium.

MIC of 0.156 μM, which was a 4-fold increase compared to that of the control. This result showed that *Lm*FabI, like *Sa*FabI, was completely inhibited by AFN-1252. In contrast, strain ANS1 expressing the *Lm*FabK1 gene was unaffected by AFN-1252 up to 50 μM, demonstrating that this FabK was able to fully support growth and was resistant to AFN-1252, as expected. The cells expressing *Lm*FabL grew poorly in the presence of greater than 0.039 μM AFN-1252, showing that while resistant to AFN-1252, *Lm*FabL was not sufficient to support a normal rate of *E. coli* growth. Therefore, FabL cannot substitute for the enoyl-acyl carrier protein reductase of type II bacterial fatty acid synthesis. Together, these experiments showed that the *L. monocytogenes* genome encoded an *Lm*FabI that was completely inhibited by AFN-1252 as well as an *Lm*FabK1 that was resistant to AFN-1252.

AFN-1252 inhibited *L. monocytogenes* growth and fatty acid synthesis. The effect of increasing concentrations of AFN-1252 on the growth rate of *L. monocytogenes* in planktonic culture was measured to determine the contribution of *Lm*FabI versus *Lm*FabK1 to fatty acid synthesis and growth. AFN-1252 caused the cessation of cell growth after 1 to 2 cellular doublings in bacterial genes encoding a single, essential FabI (24, 38). In contrast, increasing concentrations of AFN-1252 slowed but did not stop

the growth of *L. monocytogenes* (Fig. 3A). Pathway labeling experiments showed that AFN-1252 selectively inhibited lipid synthesis, with minimal perturbation to protein, DNA, and RNA synthesis (Fig. 3B). Therefore, the reduction of growth rate by AFN-1252 was attributed to on-target inhibition of *Lm*FabI and fatty acid synthesis.

The incorporation of [^{14}C]acetate into the phospholipid fraction at increasing concentrations of AFN-1252 was measured to determine the fraction of fatty acid synthesis that was inhibited by AFN-1252. Increasing concentrations of AFN-1252 caused a dose-dependent inhibition of [^{14}C]acetate incorporation, but there was a residual 20% [^{14}C]acetate incorporation that could not be eliminated by AFN-1252 (Fig. 3C). This result showed that in the absence of *Lm*FabI, *Lm*FabK1 was only able to support 20% of the normal fatty acid synthesis rate during planktonic growth. Together, these experiments point to *Lm*FabI as the enoyl-acyl carrier protein reductase dedicated to type II bacterial fatty acid synthesis, but the *Lm*FabK1 was expressed and active in *L. monocytogenes*.

Exogenous fatty acid metabolism in *L. monocytogenes*. *L. monocytogenes* is predicted to encode a fatty kinase system as in *S. aureus* for the incorporation of exogenous fatty acids (Fig. 1) (13,

14). In this system, exogenous fatty acids are phosphorylated by FakA/FakB to make acyl-phosphates (12), which can then enter phospholipid synthesis (10). The acyl-phosphate can be used by the glycerol-3-phosphate acyltransferase (PlsY) to make lysophosphatidic acid. The acyl-phosphate can also be converted into acyl-ACP by PlsX. The resulting acyl-ACP can undergo additional elongation cycles or be used by the 1-acyl-*sn*-glycerol-3-phosphate acyltransferase PlsC to make phosphatidic acid, the common precursor to phospholipid synthesis in bacteria. Genes encoding alternative pathways of exogenous fatty acid incorporation, such as acyl-ACP or acyl-CoA synthetase, were not found in the *L. monocytogenes* genome. β-Oxidation genes for breaking down fatty acids also were not found in the *L. monocytogenes* genome, so the only known fate of exogenous fatty acids is incorporation into the phospholipids.
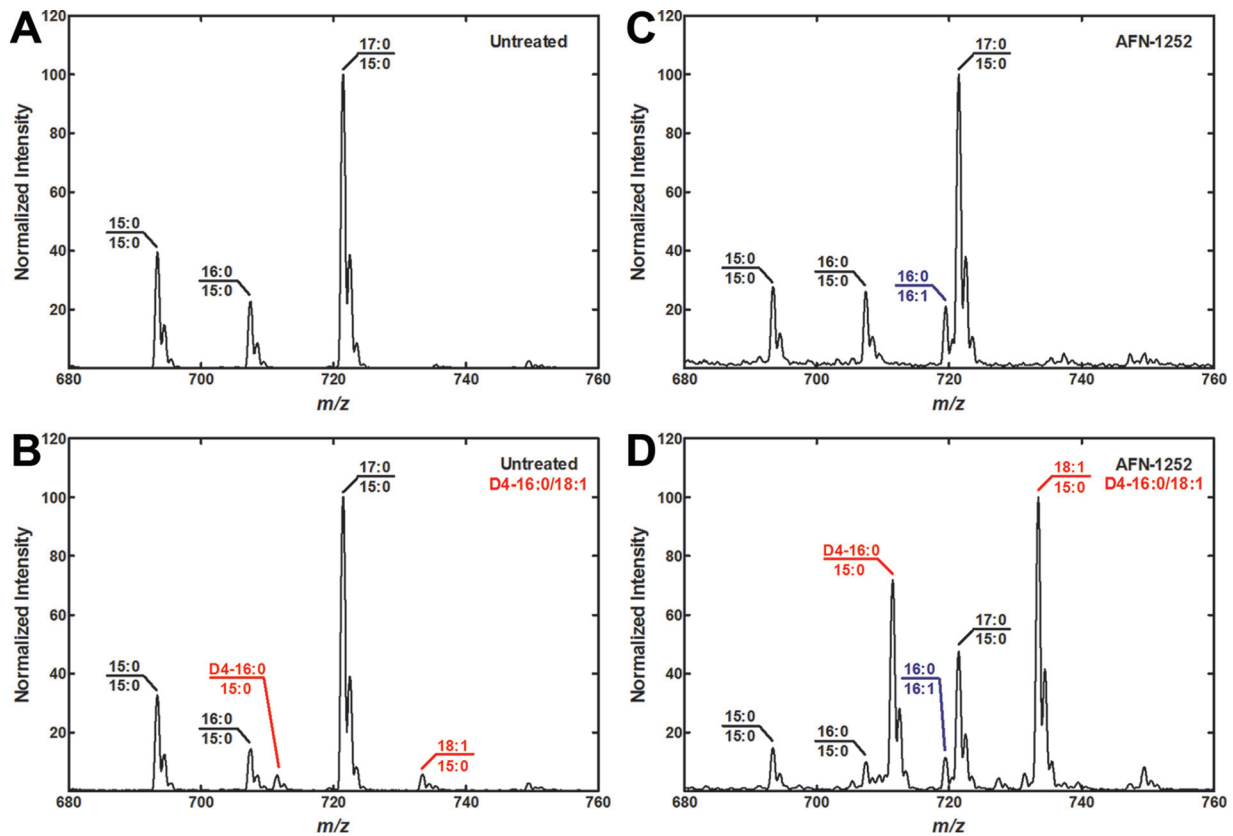
Untreated and AFN-1252-treated *L. monocytogenes* organisms were supplemented with two combinations of fatty acids to determine if exogenous fatty acids bypassed the effect of AFN-1252 inhibition. The straight-chain combination contained 100 μM D4-16:0 and 100 μM 18:1, which corresponded to two abundant fatty acid species found in mammalian serum and cellular phospholipids. This combination of fatty acids allowed the determination of whether host fatty acids can bypass FabI inhibition in *L. monocytogenes*. The deuterium-labeled D4-16:0 fatty acids have a greater mass than *L. monocytogenes*-synthesized 16:0 fatty acid, so the uptake of D4-16:0 can be monitored using mass spectrometry. The 18:1 fatty acid can be monitored without isotopic labeling because *L. monocytogenes* cannot synthesize unsaturated fatty acids (3, 5, 8, 40), so all of the incorporated 18:1 must be exogenous in origin. The branched-chain combination contained 100 μM anteiso-15:0 and 100 μM anteiso-17:0. Branched-chain fatty acids are not found in mammalian hosts but are the normal acyl chains found in *L. monocytogenes* phospholipids. *L. monocytogenes* requires branched-chain fatty acids for optimum growth (5). The branched-chain combination was intended to test if the fatty acids found in *L. monocytogenes* phospholipids can overcome FabI inhibition. Neither fatty acid combination altered the growth rate of untreated *L. monocytogenes* (Fig. 3D). Both fatty acid combinations increased the growth rate of AFN-1252-treated *L. monocytogenes* but did not restore wild-type growth rates. These data suggested that the reduction in growth rate by AFN-1252 could be partially overcome if *L. monocytogenes* was able to access host fatty acids.

The acyl chain composition of *L. monocytogenes* phospholipids was determined to verify that the exogenous fatty acids affected growth through incorporation into *L. monocytogenes* phospholipids. Molecular species analysis was performed on the phosphatidylglycerol (PG) of *L. monocytogenes*. Only the straight-chain combination was analyzed, because the anteiso-17:0 and anteiso-15:0 supplementation produced the exact same molecular species normally found in *L. monocytogenes*. The PG major molecular species in untreated *L. monocytogenes* consisted of 17:0/15:0 with smaller amounts of 15:0/15:0 and 16:0/15:0 (Fig. 4A). Only small amounts of exogenous fatty acids were incorporated into the phospholipids of untreated *L. monocytogenes*, illustrating the inefficient uptake of fatty acids by *L. monocytogenes* (Fig. 4B). Both the D4-16:0 and 18:1 species were paired with the endogenously synthesized anteiso-15:0 to give D4-16:0/15:0 and 18:1/15:0 PG molecular species. These mass spectra showed that *L. monocytogenes* genes encoded the ability to incorporate exogenous fatty acids, but this pathway made a minor contribution to phospholipid synthesis when type II bacterial fatty acid synthesis was active. The acyl chain composition of AFN-1252-treated *L. monocytogenes* was similar to that of untreated *L. monocytogenes*, with a low-abundance, new molecular species of 16:0/16:1 appearing (Fig. 4C). The 16:1 fatty acid was a component of the complex medium used in these experiments, because the *L. monocytogenes* genome does not encode the ability to synthesize unsaturated fatty acids (3, 5, 8, 40). The D4-16:0/15:0 and 18:1/15:0 combinations became major molecular species in fatty acid-supplemented, AFN-1252-treated *L. monocytogenes*, while the 17:0/15:0, 15:0/15:0, and 16:0/15:0 combinations from endogenous synthesis were reduced (Fig. 4D). Bacteria synthesizing branched-chain fatty acids have been characterized as having high selectivity for anteiso-15:0 fatty acids in the 2-position of their phospholipids and low acyl chain selectivity for the 1-position (38, 41, 42). The mass spectra showed that serum fatty acid species replaced the fatty acids at the 1-position of *L. monocytogenes* phospholipids, but the 2-position has retained high selectivity for endogenously synthesized anteiso-15:0. Together, these experiments showed that *L. monocytogenes* did not incorporate significant amounts of exogenous fatty acids when type II bacterial fatty acid synthesis was operational. Exogenous fatty acid incorporation was more pronounced when endogenous fatty acid synthesis was inhibited.

The ability to use exogenous fatty acids to replace endogenously synthesized fatty acids varies by bacterial species (12). *Streptococcus* and *Neisseria* both use straight-chain and unsaturated fatty acids, which are abundant in mammalian hosts, to make their phospholipids. Genes of both species also encode the ability to incorporate exogenous fatty acids. *Streptococcus* shuts down endogenous fatty acid synthesis in the presence of exogenous fatty acids and therefore can overcome type II bacterial fatty acid synthesis inhibition (38, 43). In contrast, *Neisseria* cannot overcome type II bacterial fatty acid synthesis inhibition despite its genes encoding the ability to incorporate exogenous fatty acids (24). The low levels of exogenous fatty acid incorporation when type II bacterial fatty acid synthesis was active, coupled with the inability of exogenous fatty acids to fully restore the growth rate of *L. monocytogenes* when FabI is inhibited, suggests that *L. monocytogenes* cannot efficiently use exogenous fatty acids to support growth. These results raised the question of whether the fatty acids found in the host cell cytosol are able to relieve FabI inhibition for intracellular *L. monocytogenes* growth.

AFN-1252 inhibited the intracellular growth of *L. monocytogenes*. The effect of AFN-1252 on the intracellular growth of *L. monocytogenes* was determined in a HeLa cell infection model (44, 45). AFN-1252 has been used previously in the intracellular infection model of *Chlamydia trachomatis* and showed no toxic effects against HeLa cells (18). The total number of intracellular *L. monocytogenes* organisms in HeLa cells was determined by lysing the infected HeLa cells and plating the lysate in serial dilutions. The number of *L. monocytogenes* CFU increased exponentially in untreated HeLa cells, with 1,300 times the initial number of CFU at 44 h (Fig. 5A). In contrast, the number of *L. monocytogenes* CFU increased initially for 2 to 3 doublings in AFN-1252-treated HeLa cells before decreasing over time (Fig. 5A). The reduction in *L. monocytogenes* titer under AFN-1252 treatment was corroborated using immunofluorescence microscopy (Fig. 5B to D) and lipid mass spectrometry (Fig. 5E and F). Untreated and AFN-1252-treated samples at 20 h after infection were stained with anti-*L.*

FIG 4 Exogenous fatty acid metabolism in *L. monocytogenes*. Growing cultures of untreated or AFN-1252 (50 μM)-treated *L. monocytogenes* in tryptic soy broth medium were not supplemented with exogenous fatty acids or were supplemented with straight-chain fatty acid (100 μM D4-16:0 and 100 μM 18:1) and grown to an A_{600} of ≈1.5. The lipids were harvested from the cells and the PG molecular species were determined. The identities of the major molecular species are annotated in the figure, and the new molecular species arising from the incorporation of the fatty acid supplements are highlighted in red. New molecular species (16:0/16:1) arising from incorporation of fatty acids present in tryptic soy broth are highlighted in blue. Spectra shown are representative examples from two biological replicates. (A) PG molecular species profile of *L. monocytogenes* with no drug treatment and no fatty acid supplementation. (B) PG molecular species profile of *L. monocytogenes* with no drug treatment and straight-chain fatty acid supplementation. (C) PG molecular species profile of *L. monocytogenes* with AFN-1252 treatment and no fatty acid supplementation. (D) PG molecular species profile of *L. monocytogenes* with AFN-1252 treatment and straight-chain fatty acid supplementation.

monocytogenes antibody and DAPI for the host cell nuclei. AFN-1252 treatment caused a 26-fold reduction in the number of *L. monocytogenes* cells (green) observed per HeLa cell (DAPI staining, blue) (Fig. 5B to D). The decrease in *L. monocytogenes* cells caused by AFN-1252 inhibition observed via microscopy corroborated the decrease observed through plating the infected HeLa cell lysate, demonstrating that AFN-1252 inhibited the intracellular replication of *L. monocytogenes*.

Molecular species analysis of the PG was also performed on untreated and AFN-1252-treated samples at 20 h after infection. A loss scan of 241 molecular weight was conducted to identify phospholipid species containing 15:0 fatty acids or inositol head groups. This method allowed the detection of only the *L. monocytogenes*-synthesized phospholipids, along with host cell phosphatidylinositol for comparison, and ignored the most abundant host phospholipid species present in the sample. The 17:0/15:0, 15:0/15:0, and 16:0/15:0 combinations were the major PG species in *L. monocytogenes*-infected HeLa cells (Fig. 5E), showing that the acyl chain composition of *L. monocytogenes* remained the same in intracellular and planktonic growth, and that intracellular *L. monocytogenes* did not incorporate significant amounts of exogenous fatty acids like in normal planktonic growth. These molecular spe-

cies peaks were significantly reduced relative to those of the host phosphatidylinositol species in the AFN-1252-treated infected HeLa cells (Fig. 5F), demonstrating that AFN-1252 inhibited intracellular *L. monocytogenes* fatty acid and phospholipid synthesis.

The effect of AFN-1252 on the *L. monocytogenes* invasion cycle was characterized by immunofluorescence microscopy through staining for both *L. monocytogenes* (green) and cellular actin (red). In a normal invasion cycle, extracellular *L. monocytogenes* is initially phagocytized into the lysosome (1). Listeriolysin O produced by *L. monocytogenes* dissolves the lysosome and allows *L. monocytogenes* to enter the cytosol, where it recruits actin and replicates (46). Intracellular *L. monocytogenes* can use the polymerization of host actin to move intracellularly or spread extracellularly. *L. monocytogenes* cells colocalized with actin represent cytosolic bacteria, while *L. monocytogenes* cells not colocalized with actin represent extracellular or lysosomal *L. monocytogenes*. *L. monocytogenes* organisms appeared as short green rods in untreated *L. monocytogenes*-infected HeLa cells at 20 h postinfection (Fig. 6A). Some of the rods colocalized with actin (red stain), consistent with these bacteria residing in the cytosol. Many of the cytosolic *L. monocytogenes* cells appeared as longer, diploid-like rods, consistent with these bacteria undergoing cell division in the
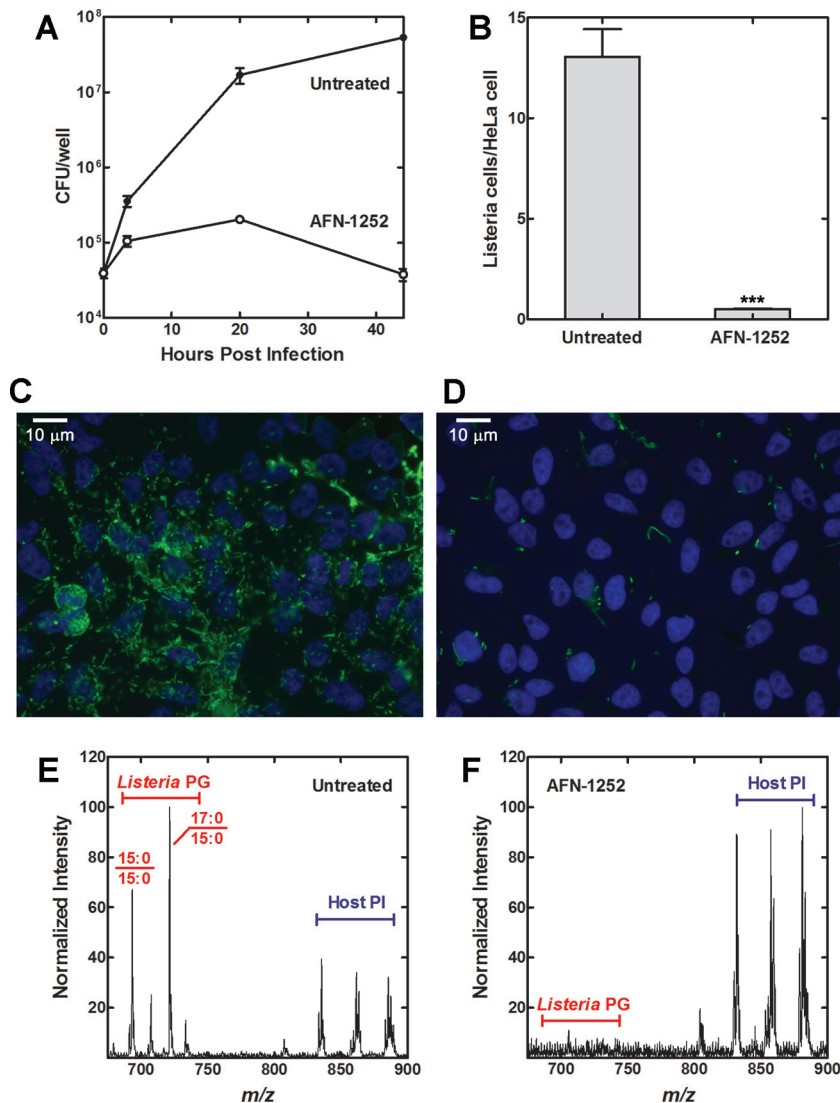
FIG 5 AFN-1252 inhibits the intracellular growth of *L. monocytogenes*. (A) Growth curve of untreated or AFN-1252 (50 μM)-treated intracellular *L. monocytogenes* in HeLa cells. (B) *L. monocytogenes*-infected HeLa cells were stained with DAPI and anti-*Listeria* antibody. Shown are the average numbers of *L. monocytogenes* organisms per HeLa cell counted from three sets of representative fields containing at least 100 HeLa cells of untreated and AFN-1252-treated *L. monocytogenes*. Significance was determined using Student's *t* test. ***, $P < 0.001$. (C) Immunofluorescence image of untreated HeLa cells infected with *L. monocytogenes* at 20 h postinfection. DAPI (blue) stain was used for the HeLa cell nucleus. Anti-*Listeria* antibody (green) stains for *L. monocytogenes*. (D) Immunofluorescence image of AFN-1252-treated HeLa cells infected with *L. monocytogenes* at 20 h postinfection. (E) Molecular species profile of lipids containing a 15:0 fatty acid or the inositol head group (loss of 241) for the untreated *L. monocytogenes*-infected HeLa cells. (F) Molecular species profile of lipids containing a 15:0 fatty acid or the inositol head group (loss of 241) for the AFN-1252-treated *L. monocytogenes*-infected HeLa cells.

cytosol. Abnormally long rods colocalizing with actin were observed in AFN-1252-treated, *L. monocytogenes*-infected HeLa cells at 20 h postinfection (Fig. 6B). The lengths of the bacteria under both conditions were quantified using ImageJ software (Fig. 7). Listeria cells under normal intracellular growth conditions were 3.1 ± 1.3 μm long, and in the presence of AFN-1252 they were 4.6 ± 3.4 μm. The large standard error was due to the bimodal distribution of cell lengths in the AFN-1252-treated cells, with many cells being considerably longer and shorter than normal. This phenotype suggested that these bacteria were unable to properly divide due to the on-target inhibition of fatty acid synthesis.

AFN-1252 caused the cessation of cellular growth after 1 to 2 cellular doublings in bacterial genomes encoding a single, essential FabI,

such as those of *Neisseria* and *Staphylococcus* (24, 38). A similar phenotype was observed in intracellular *L. monocytogenes*, where *L. monocytogenes* is able to grow for 2 to 3 doublings before cell growth stopped and the number of CFU slowly decreased over time (Fig. 5A). This result showed that *Lm*FabI was essential for the proper intracellular replication and division of *L. monocytogenes*, and that *Lm*FabK1 and exogenous fatty acid incorporation were unable to support intracellular growth. The slow decrease of *L. monocytogenes* titer from 20 h to 44 h in AFN-1252-treated cells suggested that arrested cells eventually became nonviable. Whether this is through the direct effect of the inhibitor on the viability of the bacteria or the clearing of the improperly dividing bacteria with lipid-deficient membrane by the host cell remains to be determined.
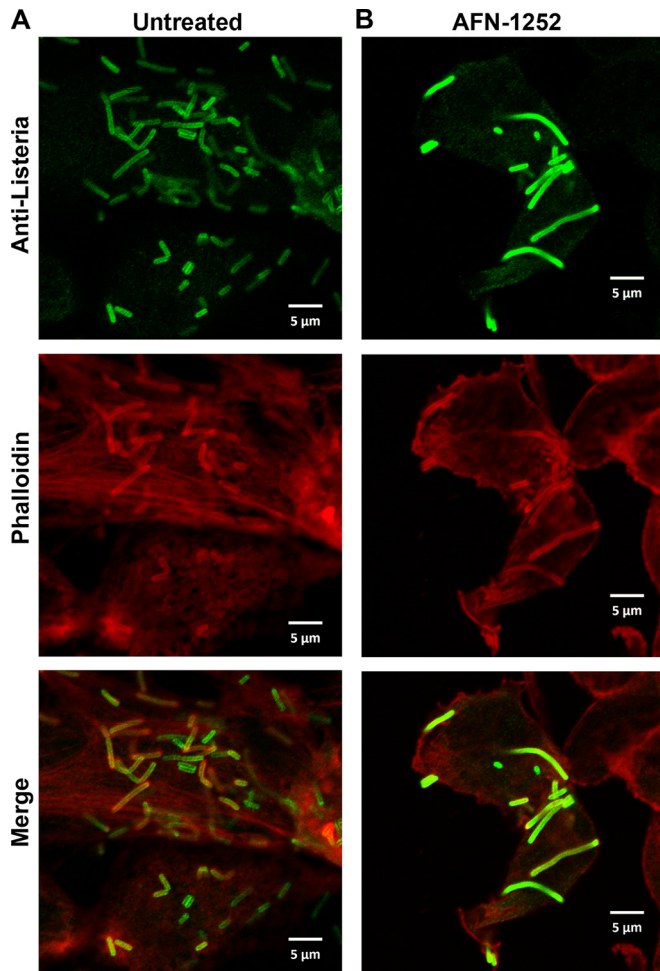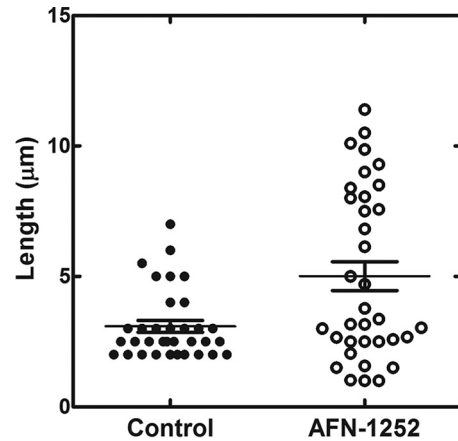
FIG 6 AFN-1252 arrested the division of intracellular *L. monocytogenes. L. monocytogenes*-infected HeLa cells were labeled with anti-*Listeria*-specific rabbit IgG antibodies, Alexa Fluor 488 (green)-conjugated goat anti-rabbit IgG, and Alexa Fluor 594 (red)-conjugated phalloidin. (Top) *L. monocytogenes* staining (green). (Middle) Cellular actin staining (red). (Bottom) Merges of the two images from the top and middle. (A) Untreated HeLa cells infected with *L. monocytogenes* for 20 h. (B) AFN-1252 (50 μM)-treated HeLa cells infected with *L. monocytogenes* for 20 h.

FIG 7 Length distribution of untreated and AFN-1252-treated *L. monocytogenes* in the intracellular infection model. The lengths of the intracellular *L. monocytogenes* cells were determined using the analyze/measure function in ImageJ software.

DISCUSSION

This study shows that FabI is the principal enoyl-ACP reductase of *L. monocytogenes* FASII and is required for the intracellular growth of this facultative intracellular pathogen. Inactivation of *Lm*FabI caused an 80% decrease in fatty acid synthesis. Although *Lm*FabK1 is capable of complementing FASII when expressed in the heterologous *E. coli* system, the physiological level of *Lm*FabK1 expression in *L. monocytogenes* can only support 20% of FASII activity in the absence of FabI. This leads to a reduced growth rate of planktonic cultures treated with AFN-1252 to inactivate FabI. Exogenous fatty acids can partially offset the growth-inhibitory effects of AFN-1252 in planktonic culture and are incorporated into membrane phospholipids, showing that the growth defect is due to reduced FASII activity. However, FabI inactivation with AFN-1252 had a more drastic effect on the intracellular growth of *L. monocytogenes*. The bacterial cells became unusually elongated, failed to divide, and eventually were cleared

from the cells. In this physiological context, neither *Lm*FabK1 expression nor the acquisition of host cell fatty acids could support *L. monocytogenes* proliferation when *Lm*FabI is inactivated. These results show that inhibitors of FabI, or any other enzyme in FASII (Fig. 1), would be effective in preventing intracellular *L. monocytogenes* replication.

L. monocytogenes does not actively incorporate exogenous fatty acids into its membrane phospholipids. The *L. monocytogenes* genome encodes the fatty acid kinase system, which is the first step in exogenous fatty acid incorporation (Fig. 1). However, the primary purpose of this system does not appear to be the incorporation of exogenous fatty acids. Exogenous fatty acids incorporated via the fatty acid kinase system constitute half the total membrane phospholipid fatty acids in *S. aureus* (14), but exogenous fatty acids only contribute a few percent to the membrane of *L. monocytogenes* during planktonic growth. Incorporation of exogenous fatty acids became significant only when fatty acid synthesis is blocked by AFN-1252. However, this enhanced exogenous fatty acid incorporation did not completely rescue the growth defect caused by FabI inhibition during planktonic growth. Incorporation of the host cell fatty acids was not able to overcome FASII inhibition in the context of intracellular growth, demonstrating that the *L. monocytogenes* fatty acid kinase system is not able to use host fatty acids to support growth. The correct acyl chain composition has been clearly demonstrated to play a key role in the environmental and intracellular survival of *L. monocytogenes*, and increasing the straight-chain composition reduces the fitness of the organism (2–6). Furthermore, fatty acids, particularly branched chains, are inhibitors of *L. monocytogenes* growth (22). In *S. aureus*, the fatty acid kinase system is used to sense the environment and acts as the master regulator of virulence, in addition to its role in the incorporation of exogenous fatty acids (14). Further work is needed to determine if the fatty acid kinase system functions in virulence signaling in *L. monocytogenes*.

ACKNOWLEDGMENTS

REFERENCES

1. **Ireton K.** 2013. Molecular mechanisms of cell-cell spread of intracellular bacterial pathogens. Open Biol **3:**130079. http://dx.doi.org/10.1098/rsob.130079.

2. **Sun Y, Wilkinson BJ, Standiford TJ, Akinbi HT, O'Riordan MXD.** 2012. Fatty acids regulate stress resistance and virulence factor production for *Listeria monocytogenes*. J Bacteriol **194:**5274–5284. http://dx.doi.org/10.1128/JB.00045-12.

3. **Zhu K, Ding X, Julotok M, Wilkinson BJ.** 2005. Exogenous isoleucine and fatty acid shortening ensure the high content of anteiso-C15:0 fatty acid required for low-temperature growth of *Listeria monocytogenes*. Appl Environ Microbiol **71:**8002–8007. http://dx.doi.org/10.1128/AEM.71.12.8002-8007.2005.

4. **Sun Y, O'Riordan MXD.** 2010. Branched-chain fatty acids promote *Listeria monocytogenes* intracellular infection and virulence. Infect Immun **78:**4667–4673. http://dx.doi.org/10.1128/IAI.00546-10.

5. **Zhu K, Bayles DO, Xiong A, Jayaswal RK, Wilkinson BJ.** 2005. Precursor and temperature modulation of fatty acid composition and growth of *Listeria monocytogenes* cold-sensitive mutants with transposon-interrupted branched-chain a-keto acid dehydrogenase. Microbiology **151:**615–623. http://dx.doi.org/10.1099/mic.0.27634-0.

6. **Lucic D, Huang ZH, Gu D, Subbaiah PV, Mazzone T.** 2007. Cellular sphingolipids regulate macrophage apolipoprotein E secretion. Biochemistry **46:**11196–11204. http://dx.doi.org/10.1021/bi701106v.

7. **Rock CO, Jackowski S.** 2002. Forty years of fatty acid biosynthesis. Biochem Biophys Res Commun **292:**1155–1166. http://dx.doi.org/10.1006/bbrc.2001.2022.

8. **Singh VK, Hattangady DS, Giotis ES, Singh AK, Chamberlain NR, Stuart MK, Wilkinson BJ.** 2008. Insertional inactivation of branched-chain a-keto acid dehydrogenase in *Staphylococcus aureus* leads to decreased branched-chain membrane fatty acid content and increased susceptibility to certain stresses. Appl Environ Microbiol **74:**5882–5890. http://dx.doi.org/10.1128/AEM.00882-08.

9. **Singh AK, Zhang Y-M, Zhu K, Subramanian C, Li Z, Jayaswal RK, Gatto C, Rock CO, Wilkinson BJ.** 2009. FabH selectivity for anteiso branched-chain fatty acid precursors in low temperature adaptation in *Listeria monocytogenes*. FEMS Microbiol Lett **301:**188–192. http://dx.doi.org/10.1111/j.1574-6968.2009.01814.x.

10. **Yao J, Rock CO.** 2013. Phosphatidic acid synthesis in bacteria. Biochim Biophys Acta **1831:**495–502. http://dx.doi.org/10.1016/j.bbalip.2012.08.018.

11. **Lu Y-J, Zhang Y-M, Grimes KD, Qi J, Lee RE, Rock CO.** 2006. Acyl-phosphates initiate membrane phospholipid synthesis in gram-positive pathogens. Mol Cell **23:**765–772. http://dx.doi.org/10.1016/j.molcel.2006.06.030.

12. **Yao J, Rock CO.** 2015. How bacterial pathogens eat host lipids: implications for the development of fatty acid synthesis therapeutics. J Biol Chem **290:**5940–5946. http://dx.doi.org/10.1074/jbc.R114.636241.

13. **Parsons JB, Frank MW, Jackson P, Subramanian C, Rock CO.** 2014. Incorporation of extracellular fatty acids by a fatty acid kinase-dependent pathway in *Staphylococcus aureus*. Mol Microbiol **92:**234–245. http://dx.doi.org/10.1111/mmi.12556.

14. **Parsons JB, Broussard TC, Bose JL, Rosch JW, Jackson P, Subramanian C, Rock CO.** 2014. Identification of a two-component fatty acid kinase responsible for host fatty acid incorporation by *Staphylococcus aureus*. Proc Natl Acad Sci U S A **111:**10532–10537. http://dx.doi.org/10.1073/pnas.1408797111.

15. **Heath RJ, Su N, Murphy CK, Rock CO.** 2000. The enoyl-[acyl-carrier-protein] reductases FabI and FabL from *Bacillus subtilis*. J Biol Chem **275:**40128–40133. http://dx.doi.org/10.1074/jbc.M005611200.

16. **Marrakchi H, DeWolf WE, Jr, Quinn C, West J, Polizzi BJ, So CY, Holmes DJ, Reed SL, Heath RJ, Payne DJ, Rock CO, Wallis NG.** 2003. Characterization of *Streptococcus pneumoniae* enoyl-[acyl carrier protein] reductase (FabK). Biochem J **370:**1055–1062. http://dx.doi.org/10.1042/bj20021699.

17. **Zhu L, Bi H, Ma J, Hu Z, Zhang W, Cronan JE, Wang H.** 2013. The two functional enoyl-acyl carrier protein reductases of *Enterococcus faecalis* do not mediate triclosan resistance. mBio **4:**e00613. http://dx.doi.org/10.1128/mBio.00613-13.

18. **Yao J, Abdelrahman YM, Robertson RM, Cox JV, Belland RJ, White SW, Rock CO.** 2014. Type II fatty acid synthesis is essential for the replication of *Chlamydia trachomatis*. J Biol Chem **289:**22365–22376. http://dx.doi.org/10.1074/jbc.M114.584185.

19. **Paoletti L, Lu Y-J, Schujman GE, de Mendoza D, Rock CO.** 2007. Coupling of fatty acid and phospholipid synthesis in *Bacillus subtilis*. J Bacteriol **189:**5816–5824. http://dx.doi.org/10.1128/JB.00602-07.

20. **Yao J, Maxwell JB, Rock CO.** 2013. Resistance to AFN-1252 arises from missense mutations in *Staphylococcus aureus* enoyl-acyl carrier protein reductase (FabI). J Biol Chem **288:**36261–36271. http://dx.doi.org/10.1074/jbc.M113.512905.

21. **Morosky S, Lennemann NJ, Coyne CB.** 2016. BPIFB6 regulates secretory pathway trafficking and enterovirus replication. J Virol **90:**5098–5107. http://dx.doi.org/10.1128/JVI.00170-16.

22. **Wang LL, Johnson EA.** 1992. Inhibition of *Listeria monocytogenes* by fatty acids and monoglycerides. Appl Environ Microbiol **58:**624–629.

23. **Parsons JB, Yao J, Frank MW, Jackson P, Rock CO.** 2012. Membrane disruption by antimicrobial fatty acids releases low molecular weight proteins from *Staphylococcus aureus*. J Bacteriol **194:**5294–5304. http://dx.doi.org/10.1128/JB.00743-12.

24. **Yao J, Bruhn DF, Frank MW, Lee RE, Rock CO.** 2016. Activation of exogenous fatty acids to acyl-acyl carrier protein cannot bypass FabI inhibition in *Neisseria*. J Biol Chem **291:**171–181. http://dx.doi.org/10.1074/jbc.M115.699462.

25. **Bligh EG, Dyer WJ.** 1959. A rapid method of total lipid extraction and purification. Can J Biochem Physiol **37:**911–917. http://dx.doi.org/10.1139/o59-099.

26. **Yao J, Dodson VJ, Frank MW, Rock CO.** 2015. *Chlamydia trachomatis* scavenges host fatty acids for phospholipid synthesis via an acyl-acyl carrier protein synthetase. J Biol Chem **290:**22173. http://dx.doi.org/10.1074/jbc.M115.671008.

27. **Francis M, Thomas CJ.** 1996. Effect of multiplicity of infection on *Listeria monocytogenes* pathogenicity for HeLa and Caco-2 cell lines. J Med Microbiol **45:**323–330. http://dx.doi.org/10.1099/00222615-45-5-323.

28. **Köprülü AD, Kastner R, Wienerroither S, Lassnig C, Putz EM, Majer O, Reutterer B, Sexl V, Kuchler K, Mnller M, Decker T, Ellmeier W.** 2013. The tyrosine kinase Btk regulates the macrophage response to *Listeria monocytogenes* infection. PLoS One **8:**e60476. http://dx.doi.org/10.1371/journal.pone.0060476.

29. **Kastner R, Dussurget O, Archambaud C, Kernbauer E, Soulat D, Cossart P, Decker T.** 2011. LipA, a tyrosine and lipid phosphatase involved in the virulence of *Listeria monocytogenes*. Infect Immun **79:**2489–2498. http://dx.doi.org/10.1128/IAI.05073-11.

30. **Bergler H, Fuchsbichler S, Högenauer G, Turnowsky F.** 1996. The enoyl-[acyl-carrier-protein] reductase (FabI) of *Escherichia coli*, which catalyzes a key regulatory step in fatty acid biosynthesis, accepts NADH and NADPH as cofactors and is inhibited by palmitoyl-CoA. Eur J Biochem **242:**689–694. http://dx.doi.org/10.1111/j.1432-1033.1996.0689r.x.

31. **Heath RJ, Rock CO.** 1995. Enoyl-acyl carrier protein reductase (*fabI*) plays a determinant role in completing cycles of fatty acid elongation in *Escherichia coli*. J Biol Chem **270:**26538–26542. http://dx.doi.org/10.1074/jbc.270.44.26538.

32. **Bergler H, Wallner P, Ebeling A, Leitinger B, Fuchsbichler S, Aschauer H, Kollenz G, Högenauer G, Turnowsky F.** 1994. Protein envM is the NADH-dependent enoyl-ACP reductase *fabI* of *Escherichia coli*. J Biol Chem **269:**5493–5496.

33. **Massengo-Tiasse RP, Cronan JE.** 2008. *Vibrio cholerae fabV* defines a new class of enoyl acyl-carrier-protein reductase. J Biol Chem **283:**1308–1316. http://dx.doi.org/10.1074/jbc.M708171200.

34. **Hirschbeck MW, Kuper J, Lu H, Liu N, Neckles C, Shah S, Wagner S, Sotriffer CA, Tonge PJ, Kisker C.** 2012. Structure of the *Yersinia pestis* FabV enoyl-ACP reductase and its interaction with two 2-pyridone inhibitors. Structure **20:**89–100. http://dx.doi.org/10.1016/j.str.2011.07.019.

35. **Bergler H, Högenauer G, Turnowsky F.** 1992. Sequences of the *envM* gene and two mutated alleles in *Escherichia coli*. J Gen Microbiol **138:**2093–2100. http://dx.doi.org/10.1099/00221287-138-10-2093.

36. **Kaplan N, Albert M, Awrey D, Bardouniotis E, Berman J, Clarke T, Dorsey M, Hafkin B, Ramnauth J, Romanov V, Schmid MB, Thalakada R, Yethon J, Pauls HW.** 2012. Mode of action, *in vitro* activity, and *in vivo* efficacy of

AFN-1252, a selective antistaphylococcal FabI inhibitor. Antimicrob Agents Chemother **56:**5865–5874. http://dx.doi.org/10.1128/AAC.01411-12.

37. **Kaplan N, Awrey D, Bardouniotis E, Berman J, Yethon J, Pauls HW, Hafkin B.** 2013. In vitro activity (MICs and rate of kill) of AFN-1252, a novel FabI inhibitor, in the presence of serum and in combination with other antibiotics. J Chemother **25:**18–25. http://dx.doi.org/10.1179/1973947812Y.0000000063.

38. **Parsons JB, Frank MW, Subramanian C, Saenkham P, Rock CO.** 2011. Metabolic basis for the differential susceptibility of Gram-positive pathogens to fatty acid synthesis inhibitors. Proc Natl Acad Sci U S A **108:**15378–15383. http://dx.doi.org/10.1073/pnas.1109208108.

39. **Karlowsky JA, Kaplan N, Hafkin B, Hoban DJ, Zhanel GG.** 2009. AFN-1252, a FabI inhibitor, demonstrates a Staphylococcus-specific spectrum of activity. Antimicrob Agents Chemother **53:**3544–3548. http://dx.doi.org/10.1128/AAC.00400-09.

40. **Giotis ES, McDowell DA, Blair IS, Wilkinson BJ.** 2007. Role of branched-chain fatty acids in pH stress tolerance in *Listeria monocytogenes*. Appl Environ Microbiol **73:**997–1001. http://dx.doi.org/10.1128/AEM.00865-06.

41. **Kaneda T.** 1991. Iso- and anteiso-fatty acids in bacteria: biosynthesis, function, and taxonomic significance. Microbiol Rev **55:**288–302.

42. **Yao J, Cherian PT, Frank MW, Rock CO.** 2015. *Chlamydia trachomatis* relies on autonomous phospholipid synthesis for membrane biogenesis. J Biol Chem **290:**18874–18888. http://dx.doi.org/10.1074/jbc.M115.657148.

43. **Brinster S, Lamberet G, Staels B, Trieu-Cuot P, Gruss A, Poyart C.** 2009. Type II fatty acid synthesis is not a suitable antibiotic target for Gram-positive pathogens. Nature **458:**83–86. http://dx.doi.org/10.1038/nature07772.

44. **Tang P, Sutherland CL, Gold MR, Finlay BB.** 1998. *Listeria monocytogenes* invasion of epithelial cells requires the MEK-1/ERK-2 mitogen-activated protein kinase pathway. Infect Immun **66:**1106–1112.

45. **Weiglein I, Goebel W, Troppmair J, Rapp UR, Demuth A, Kuhn M.** 1997. *Listeria monocytogenes* infection of HeLa cells results in listeriolysin O-mediated transient activation of the Raf-MEK-MAP kinase pathway. FEMS Microbiol Lett **148:**189–195. http://dx.doi.org/10.1111/j.1574-6968.1997.tb10287.x.

46. **Hamon MA, Ribet D, Stavru F, Cossart P.** 2012. Listeriolysin O: the Swiss army knife of *Listeria*. Trends Microbiol **20:**360–368. http://dx.doi.org/10.1016/j.tim.2012.04.006.